Numerical issues and freestream behavior of the v^2-f model.

By G. Kalitzin

1. Motivation and objectives

The numerical method used to solve the equations of a turbulence model is of comparable importance to the concerns about the representation of the flow physics, as its efficiency and robustness determines the overall performance of the flow solver. The v^2-f model by Durbin (1995) has shown to reproduce mean flow and turbulence quantities accurately for a large number of turbulent flows (Durbin 1995; Parneix & Durbin 1997; Kalitzin 1999). However, the stiffness of the equations and, in particular, of the wall boundary condition that results from the strong near-wall coupling of the $\overline{v^2}$ transport equation and the elliptic relaxation equation for f, hindered its application to large scale industrial flow applications.

Lien & Durbin (1996) proposed a 'code-friendly' version of the v^2-f model. In this version, source terms have been introduced in the $\overline{v^2}$ and f equations and $f = 0$ is imposed at the wall. This model allowed a segregated solution of the turbulence field equations and it has found wide spread use in many commercial CFD codes. Although this version of the model was constructed to reproduce the results obtained with the 1995 version of the model, it has been found, that the introduced modifications lead to larger deviations in certain flow regimes. In general, the modified model predicts a delayed laminar-turbulent transition. For low-Reynolds number flows this may actually improve flow field predictions. However, the model prediction mechanism of transition is not fully understood and it is undesirable as it also affects flow predictions at high-Reynolds numbers.

In the search for robustness, Laurence *et al.* (2004) proposed another 'code-friendly' version of the v^2-f model. This model is based on the substitution of the ratio $\overline{v^2}/k$ with a variable ϕ and the alteration of the governing equation by neglecting source terms in the f-equation. The developers of this model have tested the model on channel, diffuser flow and flow over periodic hills. Results reported reproduce the results of the 1995 version of v^2-f, while retaining the easier convergence properties of this 'code-friendly' version.

Kalitzin (2002) presents a numerical scheme for the solution of the 1995 version of the v^2-f model. That scheme solves the implicit, pairwise coupled discretized equations of the model using a Diagonally Dominant Alternating Direction Implicit (DDADI) solver. For steady state computations, local time stepping is utilized for the advancement of the turbulence equations.

The present paper proposes a modification to that scheme. It is argued that the robustness of the DDADI algorithm applied to the v^2-f model can greatly be improved when local time stepping is substituted with explicit under-relaxation. The resulting scheme has some very desirable properties and shows a very efficient and robust behavior.

In addition, the paper also conducts an analysis of the freestream behavior of the v^2-f model. It is shown, that under certain flow conditions the model provides a negative solution for the turbulent kinetic energy in the freestream. This may lead to numerical instabilities if not prevented by minimum limiters for the turbulence variables. A modification of the model is proposed that eliminates this problem and no such limiters are required.

The new DDADI scheme with explicit under-relaxation is applied to the prediction of flow over a wing that generates a large wing-tip vortex. For this case, the turbulence field is strongly coupled with the mean flow. Comparisons with the model by Spalart & Allmaras (1994) reveal significant differences in the prediction of the wing-tip vortex.

2. Improvement of the solution algorithm for the v^2-f model

The v^2-f turbulence model by Durbin (1995) consists of, in addition to the usual transport equation for the turbulent kinetic energy k and dissipation ε, a transport equation for the scalar $\overline{v^2}$ and an elliptic relaxation equation for f:

$$\left.\begin{aligned}
\partial_t k + u\cdot\nabla k &= \frac{1}{\rho}\nabla\cdot[(\mu+\mu_t)\nabla k] + P_k - \varepsilon \\
\partial_t \varepsilon + u\cdot\nabla\varepsilon &= \frac{1}{\rho}\nabla\cdot[(\mu+\frac{\mu_t}{\sigma_\varepsilon})\nabla\varepsilon] + \frac{C_{\varepsilon 1}P_k - C_{\varepsilon 2}\varepsilon}{T} \\
\partial_t\overline{v^2} + u\cdot\nabla\overline{v^2} &= \frac{1}{\rho}\nabla\cdot\left[(\mu+\mu_t)\nabla\overline{v^2}\right] + kf - \frac{\varepsilon}{k}\overline{v^2} \\
f &= L^2\nabla^2 f + \frac{C_1}{T}\left[\frac{2}{3} - \frac{\overline{v^2}}{k}\right] + C_2\frac{P_k}{k}
\end{aligned}\right\} \qquad (2.1)$$

where the eddy-viscosity is defined as:

$$\nu_t = C_\mu T\overline{v^2} \qquad (2.2)$$

The stiffness of the model results mainly from the f wall boundary condition:

$$f_w = -20\nu^2\overline{v_1^2}/(\varepsilon_w y_1^4) \qquad (2.3)$$

Kalitzin (2002) describes the implementation of this model in the compressible, structured multiblock code TFLO. The model is solved in a separate set of subroutines, segregated from the mean flow. In each block, multigrid is used for the mean flow and at each multigrid cycle the model's subroutines are called on the finest grid. They return an updated value of the eddy-viscosity and turbulent kinetic energy. These two quantities are passed to the mean flow solver for the determination of the Reynolds stresses.

The model equations are solved in an implicit, pairwise coupled manner, with a cell centered finite difference scheme. The pairwise coupled solution of the field equations allows an implicit treatment of the wall boundary conditions. The implicit matrices are factorized with a DDADI scheme. The treatment of the boundary conditions as source terms prior to factorization allows an implicit treatment of the boundary conditions in each sweeping direction of the scheme, decreasing the sensitivity of the factorization scheme to the order of the sweeping directions. The diffusion terms are discretized with second order central differences. First order upwind differences are used for the discretization of the convective terms.

In Kalitzin (2002) steady state solutions are achieved by marching in time from an initial guess. The time step was determined by scaling the local time step obtained from the mean flow with a constant factor. This factor was obtained by numerical experimentation. Another way of advancing the turbulence equations is by means of implicit under-relaxation. Implicit under-relaxation is equivalent of local time stepping with the time step:

$$\Delta t = \frac{\alpha}{(1-\alpha)B} \tag{2.4}$$

where α is the relaxation parameter ($0 < \alpha < 1$). B is the diagonal element of the implicit matrix that depends on the solution and grid. The advantage of implicit under-relaxation is that the time step for the turbulence equations is determined by the numerical properties of the discretized turbulence equations rather than through mean flow criteria and numerical experimentation for the scaling factor.

However, there are some disadvantages when implicit under-relaxation is applied to the v^2-f equations. When implicit under-relaxation is employed it introduces automatically an unsteady term in the f-equation changing its elliptic nature. Following equation (2.4) it also introduces local time stepping when a constant under-relaxation parameter is used. Local time stepping has been found to worsen the convergence of the v^2-f model for certain flows with strong shock-boundary layer interaction.

A way to avoid the introduction of an unsteady term in the f-equation is to use explicit under-relaxation. Here, the solution of the discretized model (2.1) in delta-form is weighted and added to the previous iterate:

$$\phi^{n+1} = \phi^n + \alpha \Delta \phi \tag{2.5}$$

where α is again the relaxation parameter with $0 < \alpha < 1$.

Computations show that explicit under-relaxation works well when a DDADI factorization scheme is used. The factorization error, that is usually scaled by the time step, seems to have no significant impact. Further work needs to be done to assess this error.

3. Freestream solutions

In the freestream the velocity is $u = u_\infty$. By neglecting diffusion and production the equations of the model (2.1) simplify for the steady state as:

$$u_\infty \frac{\partial k}{\partial x} = -\varepsilon \tag{3.1}$$

$$u_\infty \frac{\partial \varepsilon}{\partial x} = -\frac{C_{\varepsilon 2}}{T}\varepsilon \tag{3.2}$$

$$u_\infty \frac{\partial \overline{v^2}}{\partial x} = kf - \frac{\varepsilon}{k}\overline{v^2} \tag{3.3}$$

$$f = \frac{C_1}{T}\left[\frac{2}{3} - \frac{\overline{v^2}}{k}\right] \tag{3.4}$$

The turbulence time scale is bounded at the lower end with the Kolmogorov scale as:

$$T = max\left[\frac{k}{\varepsilon}, 6\sqrt{\frac{\nu}{\varepsilon}}\right] \tag{3.5}$$

For $T = k/\varepsilon$ the analytical solutions of the differential equations (3.1)-(3.3) are:

$$k = k_0 \hat{z}^{\frac{-1}{C_{\varepsilon 2}-1}} \tag{3.6}$$

$$\varepsilon = \varepsilon_0 \hat{z}^{\frac{-C_{\varepsilon 2}}{C_{\varepsilon 2}-1}} \tag{3.7}$$

$$\overline{v^2} = k\left[\frac{2}{3} - (\frac{2}{3} - \frac{\overline{v^2}_0}{k_0})\hat{z}^{\frac{-C_1}{C_{\varepsilon 2}-1}}\right] \tag{3.8}$$

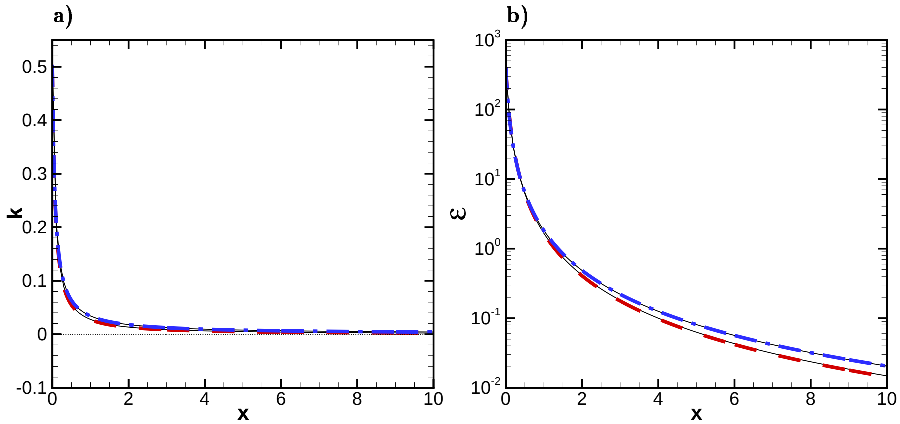

FIGURE 1. Turbulent kinetic energy (a) and dissipation (b) of convecting freestream turbulence with $T_{u,0} = 0.01$, $\nu_{t,0}/\nu = 3.6$. ---- : $T = k/\varepsilon$; —·— : $T = 6\sqrt{\nu/\varepsilon}$; —— : analytical solution.

with $\hat{z} = \frac{C_{\varepsilon 2}-1}{u_\infty}\frac{\varepsilon_0}{k_0}(x - x_0) + 1$.

For $T = 6\sqrt{\nu/\varepsilon}$ the equations (3.1)-(3.2) decouple and the analytical solutions are:

$$k = k_0 - \frac{12\sqrt{\varepsilon_0 \nu}}{C_{\varepsilon 2}}(1 - \frac{1}{\tilde{z}}) \tag{3.9}$$

$$\varepsilon = \frac{\varepsilon_0}{\tilde{z}^2} \tag{3.10}$$

$$\overline{v^2} = k\left[\frac{2}{3} - (\frac{2}{3} - \frac{\overline{v^2}_0}{k_0})\tilde{z}^{\frac{-2C_1}{C_{\varepsilon 2}}}\right] \tag{3.11}$$

with $\tilde{z} = \frac{C_{\varepsilon 2}\sqrt{\varepsilon_0}}{12 u_\infty \sqrt{\nu}}(x - x_0) + 1$. In contrast to equation (3.6), the equation (3.9) gives negative values for k for certain values of ε_0 and a computational domain that exceed a critical length.

Turbulence at the inflow boundary of the computational domain can be specified through the turbulence intensity, T_u, and the ratio of eddy to molecular viscosity, ν_{t0}/ν:

$$k_0 = \frac{3}{2}(T_u\, u_\infty)^2\ , \quad \varepsilon_0 = 0.09\beta\frac{k_0^2}{\nu_{t0}} \tag{3.12}$$

The dissipation is here specified using the standard eddy-viscosity definition and equation (2.2). The coefficient is $\beta = C_\mu \overline{v^2}_0 T_0/(0.09k_0^2/\varepsilon_0)$. In the freestream the factor β is about $\beta \approx 1.4$ assuming that $T_0 = k_0/\varepsilon_0$ and $\overline{v^2}_0 = 2k_0/3$. The coefficient C_μ is 0.19.

In equation (3.9), $\tilde{z} = 1$ for $x = x_0$. At this location, k has its maximum. The minimum of k is located at $z \to \infty$ which corresponds to $x \to \infty$. For it to be positive the initial value k_0 has to be:

$$k_0 > \frac{12\sqrt{\varepsilon_0 \nu}}{C_{\varepsilon 2}} \tag{3.13}$$

Substituting ε_0 with the relation (3.12) a minimum bound for the ratio of eddy to molecular viscosity can be derived as:

$$\frac{\nu_{t0}}{\nu} > \left(\frac{3.6}{C_{\varepsilon 2}}\right)^2 \beta \approx 3.61\beta \tag{3.14}$$

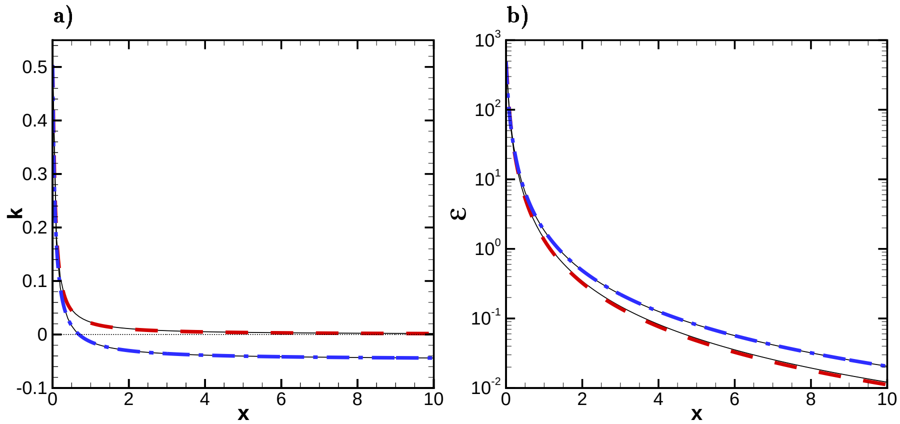

FIGURE 2. Turbulent kinetic energy (a) and dissipation (b) of convecting freestream turbulence with $T_{u,0} = 0.01$, $\nu_{t,0}/\nu = 3.0$. - - - - : $T = k/\varepsilon$; —·— : $T = 6\sqrt{\nu/\varepsilon}$; ——— : analytical solution.

This bound guarantees $k > 0$ for any x.

The solution of equations (3.6) and (3.9) are plotted in Figure 1a. The figure includes the analytical and the numerical solutions obtained by solving the full v^2-f model (2.1) for uniform flow. The chosen flow conditions are: $u_\infty = 58m/s, \nu = 1.55\,10^{-5}m^2/s, T_u = 0.01$ and $\nu_{t,0}/\nu = 3.6$. The computational domain is $10m$ long. The coefficient $C_{\varepsilon 2}$ is equal 1.9. It can be seen that the solutions for k are very similar and positive for both cases with $T = k/\varepsilon$ and $T = 6\sqrt{\nu/\varepsilon}$.

Figure 2 shows the solution for $\nu_{t,0}/\nu = 3.0$. Equation (3.9) gives now negative values for k. Comparing Figures 1b and 2b it is interesting to note the large change in k while the ε distribution (3.10) hardly changed.

It can be shown that the turbulence time scale (3.5) is eventually bounded with the Kolmogorov scale independently of the values of k_0 and ε_0 at the inflow. When $T = k/\varepsilon$, the turbulent kinetic energy is related to the dissipation following equations (3.6) and (3.7) as:

$$k = k_0 \left(\frac{\varepsilon}{\varepsilon_0}\right)^{1/C_{\varepsilon 2}} \tag{3.15}$$

The turbulence time scale, defined by equation (3.5), hits the lower bound when

$$k = 6\sqrt{\nu\varepsilon} \tag{3.16}$$

The two functions (3.15) and (3.16) intersect for

$$\varepsilon_1 = \left(\frac{\varepsilon_0^{2/C_{\varepsilon 2}} 36\nu}{k_0^2}\right)^{\frac{C_{\varepsilon 2}}{2-C_{\varepsilon 2}}} \tag{3.17}$$

The corresponding location is according equation (3.7):

$$x_1 = x_0 + \left((\frac{\varepsilon_1}{\varepsilon_0})^{\frac{1-C_{\varepsilon 2}}{C_{\varepsilon 2}}} - 1 \right) \frac{u_\infty k_0}{(C_{\varepsilon 2} - 1)\varepsilon_0} \tag{3.18}$$

Once the bound is reached, the turbulence variables are given by equations (3.9)-(3.11) whereby the values at x_1 are used as initial values.

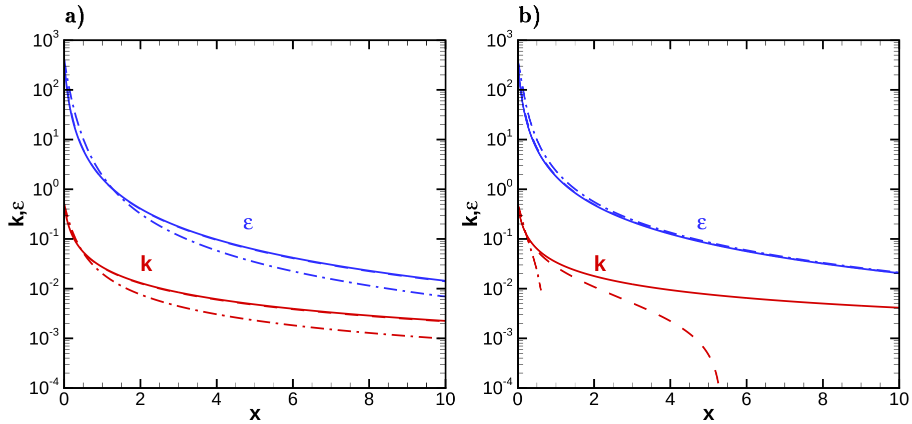

FIGURE 3. Turbulent kinetic energy and dissipation of convecting freestream turbulence with $T_{u,0} = 0.01$ and $\nu_{t,0}/\nu = 3.6$. The turbulence time scale is: a) $T = k/\varepsilon$ and b) $T = 6\sqrt{\nu/\varepsilon}$. ——— : $\Delta x = 0.0025$, 2nd order; ---- : $\Delta x = 0.025$, 1st order; —·— : $\Delta x = 0.1$, 1st order.

The behavior of $\overline{v^2}$ in the freestream is given by equations (3.8) and (3.11) for the unbounded and bounded case, respectively. Note that the variable $\overline{v^2}$ behaves like k when $\overline{v^2}_0/k_0 = 2/3$. In this case f in the freestream is identical zero.

3.1. *Discretization error*

For robustness, the convection terms are usually discretized with an upwind scheme. It can be shown that the numerical dissipation resulting from the upwind treatment of the convection terms aggravates the problem of negative turbulent kinetic energy in the freestream. For this, we analyze the transport equation for the turbulence kinetic energy in the freestream discretized for cell i with first order upwind. For $u_\infty > 0$ the discretized equation (3.1) becomes:

$$u_\infty \frac{k_i - k_{i-1}}{\Delta x} = -\varepsilon_i \tag{3.19}$$

A Taylor series expansion gives

$$k_{i-1} = k_i - \left(\frac{\partial k}{\partial x}\right)_i \Delta x - \left(\frac{\partial^2 k}{\partial x^2}\right)_i \frac{\Delta x^2}{2} \tag{3.20}$$

which leads to:

$$u_\infty \left(\frac{\partial k}{\partial x}\right)_i = -\varepsilon_i - u_\infty \left(\frac{\partial^2 k}{\partial x^2}\right)_i \frac{\Delta x}{2} \tag{3.21}$$

The second derivative of k is positive according to equation (3.9). The second term on the right hand side of equations (3.21) acts as negative source term. Results for different grids and discretizations are shown in Figure 3 for the same flow conditions as used for Figure 1. Clearly, for both time scale definitions the numerical error deteriorates the solution. However, the lack of coupling between the k and ε equation for $T = 6\sqrt{\nu/\varepsilon}$ prevents ε to decrease for lower values of k as shown for the case $T = k/\varepsilon$ in Figure 3a.

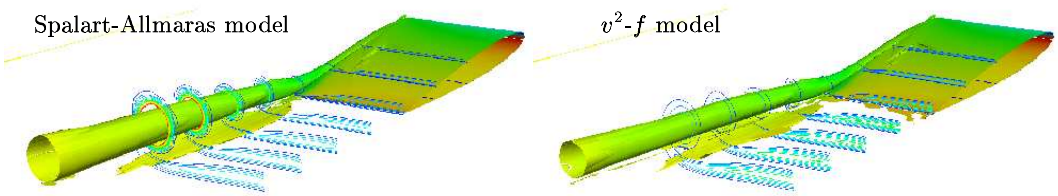

FIGURE 4. Wing-tip vortex visualized with λ_2-surface colored with pressure contours and eddy-viscosity contour-lines in selected planes

4. Model modification

The lower bound for the turbulence time scale has been designed by Durbin (1995) to enforce the correct asymptotic behavior of the k-ε equations near the wall. Thus it should be applied only in the near wall region. There are several ways to eliminate the lower bound in the freestream. The simplest way is to define a large value for the eddy-viscosity at the inflow. One can also define a distance from the wall which specifies the near wall region and thus the region where the limiter (3.5) is active. More sophisticated solutions include the use of an interpolation function similar to that used by Durbin (1995) for the coefficient $C_{\varepsilon 1}$ or the one used by Menter (1993) for the switch between the k-ω and k-ε models. The latter two possibilities require testing to avoid the situation that the bound is not active when it is needed. At the current stage we utilize a larger ratio of ν_{t_0}/ν at the inflow.

5. Wing-tip vortex

The goal of this test case is the accurate prediction of a wing tip vortex generated by a low aspect ratio wing. The flow conditions are: $Re_c = 4.6\,10^6, M = 0.15$ and $\alpha = 10^o$ for which extensive experimental data is available by Dacles-Mariani *et al.* (1995). To reduce the influence of the inflow and outflow boundaries, the computational domain has been extended both upstream and downstream by one cord length. The wall normal grid spacing is such that $y^+ < 0.5$. The wind tunnel walls are treated as inviscid walls to reduce the grid size. The computations were carried out with TFLO with a low dissipative Roe's approximate Riemann solver in combination with a second order reconstruction scheme and several turbulence models.

Preliminary results obtained with the Spalart-Allmaras and v^2-f turbulence models are shown in Figure 4. The wing-tip vortex is visualized with a $\lambda_2 \approx 0$ surface as described by Jeong & Hussain (1995). The λ_2 surface is colored with pressure contours. Eddy-viscosity contours are plotted in selected planes.

The eddy-viscosity contours show that the level of turbulence in the vortex is much less for v^2-f than for Spalart-Allmaras. The lower levels of eddy-viscosity mean that there is less diffusion in the vortex and therefore it is preserved over a longer distance. As demonstrated in Figure 4, the diameter of the vortex core grows much slower when v^2-f is used.

6. Conclusion and future work

The first part of the paper describes a modification to the DDADI scheme developed earlier by Kalitzin (2002) for the solution of the v^2-f turbulence model. A significant improvement in robustness can be achieved when explicit under-relaxation is used instead of (local) time stepping when solving the turbulence equations. The described solution algorithm makes computation with the 1995 version of Durbin's v^2-f model comparable efficient and robust as with other RANS turbulence models like the Spalart-Allmaras or Menters SST model.

The second part of the paper describes the freestream behavior of the v^2-f model. It concludes that a modification of the lower bound for the turbulence time scale is needed to prevent its use in the freestream where it may cause negative values for the turbulent kinetic energy. These may also be prevented when large values for the eddy-viscosity are specified at the inflow.

7. Acknowledgments

The flow computation of the wing-tip vortex were performed with TFLO by Edwin van der Weide. The used grid was generated by Sang Ho Kim. Gratitude is extended to Gianluca Iaccarino and Paul Durbin for their comments on the freestream analysis. The support by the US Department of Energy under the ASCI program is gratefully acknowledged.

REFERENCES

Dacles-Mariani J., Zilliac G.G., Chow J.S. and Bradshaw P 1995 Numerical/experimental study of a wingtip vortex in the near field. *AIAA J.*, **33(9)**, 1561-1570.

Durbin, P. A. 1995 Separated flow computations with the k-ε-$\overline{v^2}$ model. *AIAA J.*, **33**, 659-664.

Jeong J. and Hussain F. 1995 On the identification of a vortex. *JFM*, **285**, 6994.

Kalitzin G. 1999 Application of v^2-f turbulence model to transonic flows, *AIAA*, **99-3780**.

Kalitzin, G. 2002 An efficient and robust algorithm for the solution of the v^2-f turbulence model with application to turbomachinery flow. *WEHSFF2002*.

Laurence D., R., Uribe J., C. and Utyuzhnikov S., V. 2004 A robust formulation of the v^2-f model, *APPL*.

Lien, F. S. & Durbin, P. A. 1996 Non-linear k-ε-v^2 modeling with application to high-lift. *CTR summer proceedings*.

Menter F. R., 1993, Zonal two-equation k-ω turbulence model predictions. *AIAA*, **93-2906**.

Parneix S. & Durbin, P. A. 1997 Numerical simulation of 3D turbulent boundary layers using the V2F model, CTR-Annual Research Briefs. 135-148.

Spalart P. R. & Allmaras S. R. 1994 A one-equation turbulence model for aerodynamic flows. *La Recherche Aerospatiale*, **1**, 1-23.